

Multiplicity density at mid-rapidity in AA collisions: effect of meson cloud

B.G. Zakharov¹

¹*L.D. Landau Institute for Theoretical Physics, GSP-1, 117940, Kosygina Str. 2, 117334 Moscow, Russia*
(Dated: May 20, 2016)

We study the influence of the meson cloud of the nucleon on predictions of the Monte Carlo Glauber model for the charged particle multiplicity density at mid-rapidity in AA collisions. We find that for central AA collisions the meson cloud can increase the multiplicity density by $\sim 16 - 18\%$. The meson-baryon Fock component reduces the required fraction of the binary collisions by a factor of ~ 2 for Au+Au collisions at $\sqrt{s} = 0.2$ TeV and ~ 1.5 for Pb+Pb collisions at $\sqrt{s} = 2.76$ TeV.

PACS numbers:

I. INTRODUCTION

The understanding of the initial entropy/energy distribution is crucial for hydrodynamical simulation of the evolution of the hot quark-gluon plasma (QGP) in high-energy AA collisions. A rigorous determination of the initial conditions for the plasma fireball in AA collisions is presently impossible. The most popular methods in use for this purpose at the present time are the IP-Glasma model [1, 2] and the wounded nucleon Glauber model [3, 4]. The IP-Glasma approach is based on the pQCD color-glass condensate model [5]. Unfortunately the applicability of the pQCD in the IP-Glasma model is questionable since it assumes that gluon fields can be treated perturbatively down to an infrared scale $m \sim \Lambda_{QCD}$ [1, 2]. It is several times smaller than the inverse gluon correlation radius in the QCD vacuum $1/R_c \sim 0.75$ GeV [6], which is the natural lower limit for the virtuality scale of the perturbative gluons. In the dipole approach [7] for $m \sim 0.75$ GeV the perturbative contribution to the hadronic cross sections turns out to be smaller than the nonperturbative one up to $\sqrt{s} \sim 10^3$ GeV [8]. For this reason even at the LHC energies a purely perturbative treatment of the hadron cross sections is questionable.

The wounded nucleon Glauber model [3, 4] is a phenomenological scheme. Originally [3] it was assumed that in AA collisions each nucleon undergoing inelastic soft interaction (participant) produces a fixed contribution to the multiplicity rapidity density. At mid-rapidity ($\eta = 0$) in the c.m. frame this contribution equals half of the pp multiplicity rapidity density. It gives for AA collisions the multiplicity density $\propto N_{part}$, where N_{part} is the number of participants in both the colliding nuclei. Later, in [4] it was proposed to include in the model the contribution from hard processes that gives the particle density proportional to the number of the binary collisions N_{coll} . In this two component version the charged particle multiplicity density in AA collisions takes the form

$$\frac{dN_{ch}(AA)}{d\eta} = \frac{(1 - \alpha)}{2} n_{pp} N_{part} + \alpha n_{pp} N_{coll}, \quad (1)$$

where $n_{pp} = dN_{ch}/d\eta$ is the multiplicity density in pp collisions, and α characterizes the magnitude of hard processes to multiparticle production. In the Glauber model

model N_{part} and N_{coll} can be expressed via the inelastic pp cross section and the nuclear density. Fitting the data on the centrality dependence of the charged particle multiplicity in Au+Au collisions at $\sqrt{s} = 0.2$ TeV and in Pb+Pb collisions at 2.76 TeV gives $\alpha \approx 0.13 - 0.15$ [9–11]. For such a value of α the hard contribution to the particle production in AA collisions turns out to be rather large ($\sim 40 - 50\%$ for central collisions). It is important that the two component Glauber model allows the Monte Carlo formulation [12–14]. The Monte Carlo Glauber (MCG) model has proved to be a useful tool for analysis of the event-by-event fluctuations of observables in AA collisions.

The model of wounded nucleons has been also formulated at quark level [15, 16] when inelastic interaction of the nucleon is treated as a combination of inelastic interactions of its constituent quarks. However, in this picture the quark contribution to the multiplicity required for description of data on AA collisions may differ substantially from the one that is necessary for pp collisions [17]. Say, the data on Au+Au collisions at $\sqrt{s} = 0.2$ TeV require the quark contribution suppressed by a factor ~ 1.4 as compared to pp interaction [17]. However, the situation with consistency between AA and pp collisions becomes better if the nucleon is treated as a quark-diquark system [18].

The common feature of the wounded nucleon models with internal nucleon structure is the nonlinear increase of $dN_{ch}(AA)/d\eta$ with the number of wounded nucleons even without the hard contribution [17–20]. This is due to the growth of the fraction of the wounded constituents in each nucleon in AA collisions as compared to that in pp collisions. It is clear that a similar effect should arise from the meson cloud of the nucleon. The total weight of the meson-baryon Fock states in the nucleon may be as large as $\sim 40\%$ [21] (with the dominant contribution from the πN component). The purpose of the present work is to study within the MCG approach the possible effect of the meson-baryon component of the nucleon on the multiplicity rapidity density in AA collisions. We will analyze within the MCG model with the meson cloud data on Au+Au collisions at $\sqrt{s} = 0.2$ [22] and Pb+Pb collisions at 2.76 TeV [23].

II. THEORETICAL FRAMEWORK

At high energies the wave function of the physical nucleon becomes identical to that in the infinite momentum frame (IMF). It can be written in the form [21, 24]

$$|N\rangle_{phys} = \sqrt{1 - n_{MB}}|N\rangle + \sum_{MB} \int dx d\mathbf{k} \Psi_{MB}(x, \mathbf{k}) |MB\rangle, \quad (2)$$

where N , B , and M denote the bare baryon and meson states, x is the fractional longitudinal meson momentum in the physical nucleon, Ψ_{MB} is the probability amplitude for the MB Fock state, and

$$n_{MB} = \sum_{MB} \int dx d\mathbf{k} |\Psi_{MB}(x, \mathbf{k})|^2 \quad (3)$$

is the total weight of the MB Fock components. The energy denominator of time-ordered perturbation theory in the IMF for the MB component reads $E_N - E_M - E_B \approx [m_N^2 - M_{MB}^2(x, \mathbf{k}^2)]/2E_N$, where

$$M_{MB}^2(x, \mathbf{k}^2) = \frac{m_M^2 + \mathbf{k}^2}{x} + \frac{m_B^2 + \mathbf{k}^2}{1 - x} \quad (4)$$

is the squared invariant mass of the MB system. For the normalization corresponding to (3) the IMF wave function (for point-like particles) may be written as

$$\Psi_{MB}(x, \mathbf{k}) = \frac{\langle MB|V|N\rangle}{4\pi^{3/2} \sqrt{x(1-x)} [m_N^2 - M_{MB}^2(x, \mathbf{k})]}. \quad (5)$$

Here $\langle MB|V|N\rangle$ is the vertex factor in the IMF-limit, which depends on the form of the Lagrangian. For the dominant πN state $\langle \pi N'|V|N\rangle = g_{\pi NN'} \bar{u}_{N'} \gamma_5 u_N$ (the helicity dependent vertex functions for different MB states can be found in [21]). In phenomenological applications the internal structure of the hadrons is accounted for by multiplying the vertex factor for point-like particles by a form factor, F , which in the IMF scheme depends on x and \mathbf{k} only via $M_{MB}(x, \mathbf{k})$ [21, 24, 25].

To a good approximation one can account for in (2) only πN , $\pi \Delta$, ρN and $\rho \Delta$ two-body states [21, 25]. Since the bare Δ and ρ -meson states have the same quark content as N and π , it is reasonable to assume that their inelastic interactions are similar to that for N and π states. Then, from the point of view of the MCG model, each physical nucleon interacts with the probability $1 - n_{MB}$ as the bare N and with the probability n_{MB} as the two-body πN system. For π -meson the x -distribution is peaked at $x \sim 0.3$ and for ρ -meson at $x \sim 0.5$ [21]. For simplicity in our MCG calculations we neglect fluctuations of x and take $x = 0.3$. For the transverse spacial distribution of the MB state we use the distribution of the dominant πN component. It was renormalized to match the total weight of the MB component $n_{MB} = 0.4$ [21]. We calculated the transverse spacial distribution using the dipole formfactor [25]

$$F = \left(\frac{\Lambda^2 + m_N^2}{\Lambda^2 + M_{\pi N}^2(x, \mathbf{k})} \right)^2. \quad (6)$$

We take $\Lambda = 1.3$ GeV, such a value is supported by the data on $pp \rightarrow nX$ [26]. It gives for the mean squared transverse radius of the MB component $\langle \rho_{MB}^2 \rangle^{1/2} \approx 0.87$ fm. However, the results of the MCG simulation depends weakly on the value of Λ . This is due to the fact that in the Glauber model there is no shadowing effect for inelastic interactions.

In our model inelastic interaction of the physical nucleons from the colliding objects is a combination of $N + N$, $N + MB$, $MB + N$ and $MB + MB$ interactions. We assume that the inelastic cross sections for the bare states obey the constituent quark counting rule $4\sigma_{in}^{NN} = 6\sigma_{in}^{MB} = 9\sigma_{in}^{MM}$. For the profiles of the probability of ab inelastic interaction in the impact parameter we use a Gaussian form

$$P_{ab}(\rho) = \exp(-\pi\rho^2/\sigma_{in}^{ab}). \quad (7)$$

The value of σ_{in}^{NN} has been adjusted to reproduce the experimental inelastic pp cross section σ_{in}^{pp} (see below).

We consider the multiplicity density at $\eta = 0$ ($y = 0$). The direct data on $dN_{ch}/d\eta$ for pion-proton and pion-pion collisions for RHIC-LHC energies are absent. Calculations within the quark-gluon string scheme [27, 28] show that the charged particle multiplicity density in the central rapidity region for pion-proton and pion-pion collisions is somewhat bigger than for proton-proton collisions. To good accuracy this excess compensates a possible reduction of the multiplicity density in πN and $\pi\pi$ interactions due to somewhat smaller c.m. energy in our model. For this reason we assume that all the wounded bare particles produce the same amount of entropy per unit pseudorapidity η in the c.m. frame of colliding objects (pp or AA). We ignore the effect of a small rapidity shift (~ 0.5) of the c.m. frame for pairs with different energies (as occurs for πN interactions) on the entropy rapidity density since it is flat at mid-rapidity.

The total rapidity density for AA collisions is the sum of the contributions from the sources corresponding to the wounded constituents and to the binary collisions

$$\frac{dS}{dy} = \sum_{i=1}^{N_w} \frac{dS_w^i}{dy} + \sum_{i=1}^{N_{bin}} \frac{dS_{bin}^i}{dy}. \quad (8)$$

We write the contribution of each source from the wounded constituents as $dS_w^i/dy = \frac{(1-\alpha)}{2} S$. The contribution of each binary collision is $dS_{bin}^i/dy = S$, and for each pair of wounded particles the probability of a hard binary collision is α . We assume an isentropic expansion of the QGP. In this case the initial entropy rapidity density is proportional the charged particle pseudorapidity density $dS/dy = C dN_{ch}/d\eta$, where $C \approx 7.67$ [29]. In this approximation one can replace in (8) the entropy density by the pseudorapidity charged particle density. And the fluctuating entropy density S for each source is replaced by the fluctuating pseudorapidity charged particle density $n = S/C$. We describe the fluctuations of n by the

Gamma distribution

$$P(n, \langle n \rangle) = \left(\frac{n}{\langle n \rangle} \right)^{k-1} \frac{k^k \exp[-nk/\langle n \rangle]}{\langle n \rangle \Gamma(k)}. \quad (9)$$

The parameters $\langle n \rangle$ and k have been fitted from pp data on $dN_{ch}/d\eta$ (see below). Note however that for AA collisions the results are only weakly sensitive to fluctuations of n (except for the region of very high multiplicities).

For calculation of the centrality dependence of the charged particle multiplicity in AA collisions the distribution of the entropy rapidity density in the transverse coordinates, $\rho_s = dS/dy d\mathbf{\rho}$, is not important. However, it is necessary for calculation of geometric quantities such as the initial anisotropy ϵ_n [30]

$$\epsilon_n = \frac{\int d\mathbf{\rho} \rho^n e^{in\phi} \rho_s(\mathbf{\rho})}{\int d\mathbf{\rho} \rho^n \rho_s(\mathbf{\rho})}. \quad (10)$$

In the approximation of the point-like sources we have

$$\rho_s(\mathbf{\rho}) = \sum_{i=1}^{N_w} \delta(\mathbf{\rho} - \mathbf{\rho}_i) \frac{dS_w^i}{dy} + \sum_{i=1}^{N_{bin}} \delta(\mathbf{\rho} - \mathbf{\rho}_i) \frac{dS_{bin}^i}{dy}. \quad (11)$$

We assume that for each binary collision the source is located in the middle between colliding constituents. Physically the approximation of the point-like sources is clearly unreasonable. To account for qualitatively the finite size of the sources we replaced in our MCG code the δ functions in (11) by a Gaussian distribution $\exp(-\mathbf{\rho}^2/a_s^2)/\pi a_s^2$ with $a_s = 0.7$ fm. We observed that the results for the anisotropy coefficients ϵ_n becomes sensitive to the smearing of the sources only for very peripheral collisions.

We perform calculations using the Woods-Saxon nuclear distribution

$$\rho_A(r) = \frac{c}{1 + \exp[(r - R_A)/a]}, \quad (12)$$

where c is the normalization constant, $R_A = (1.12A^{1/3} - 0.86/A^{1/3})$ fm, $a = 0.54$ fm [14].

III. NUMERICAL RESULTS

In numerical calculations we take $n_{pp} = 2.65$ at $\sqrt{s} = 0.2$ TeV obtained by the UA1 collaboration [31]. The direct pp data on n_{pp} at $\sqrt{s} = 2.76$ TeV are absent. We obtained it with the help of the power law interpolation between the CMS data at $\sqrt{s} = 2.36$ TeV [32] ($n_{pp} = 4.47 \pm 0.04(\text{stat.}) \pm 0.16(\text{syst.})$) and at $\sqrt{s} = 7$ TeV [33] ($n_{pp} = 5.78 \pm 0.01(\text{stat.}) \pm 0.23(\text{syst.})$). It gives $n_{pp} \approx 4.65$ at $\sqrt{s} = 2.76$ TeV. The multiplicity densities measured in [31–33] correspond to the non-single-diffractive (NSD) events. For this reason in the MCG simulation one should also take for σ_{in}^{pp} the cross section corresponding to the NSD event class. The exclusion of the diffractive contribution to the inelastic cross section is

reasonable since the diffractive events do not contribute to the mid-rapidity multiplicity density.

We use for the NSD pp cross section at $\sqrt{s} = 0.2$ TeV the value 35 mb measured by the UA1 collaboration [31], and at $\sqrt{s} = 2.76$ TeV the value 50.24 mb obtained by the ALICE collaboration [34]. Making use of the above values of the NSD σ_{in}^{pp} we fitted σ_{in}^{NN} . For the scenario with meson cloud we obtained

$$\sigma_{in}^{NN}[\sqrt{s} = 0.2, 2.76 \text{ TeV}] \approx [26.15, 38.4] \text{ mb}. \quad (13)$$

In the scenario without meson cloud σ_{in}^{NN} is equal simply to the experimental NSD pp cross section. The parameters $\langle n \rangle$ and k in the Gamma distribution (9) have been fitted to reproduce the experimental n_{pp} and to satisfy the relation $n_{pp}/D = 1$ (D^2 is a variance of $dN_{ch}/d\eta$) which is well satisfied for the experimental multiplicity distribution in the pseudorapidity window $|\eta| < 0.5$ at $\sqrt{s} = 0.2$ TeV [31] and at $\sqrt{s} = 2.36$ TeV [35]. For the scenario without meson cloud $\langle n \rangle$ equals the experimental n_{pp} for any fraction of the binary collisions. For $\alpha = 0$ the relation $n_{pp}/D = 1$ gives $k = 0.5$. For nonzero α the value of k grows weakly with α , but the deviation from 0.5 is small. For the scenario with meson cloud the required value of $\langle n \rangle$ is smaller than n_{pp} , and k is close to 0.5.

We first fitted the parameters $\langle n \rangle$ and k to the pp data for set of α . Then we used them to fit the parameter α to best reproduce the data on the centrality dependence of $dN_{ch}/d\eta$ in Au+Au collisions at $\sqrt{s} = 0.2$ TeV from STAR [22] and in Pb+Pb collisions at $\sqrt{s} = 2.76$ TeV from ALICE [23]. For Au+Au collisions at $\sqrt{s} = 0.2$ TeV we obtained $\alpha \approx 0.06$ and $\alpha \approx 0.135$ for the scenarios with and without meson cloud, respectively. And for Pb+Pb collisions at $\sqrt{s} = 2.76$ TeV for these two scenarios our fits give $\alpha \approx 0.09$ and $\alpha \approx 0.14$. For the above values of α the parameters of the Gamma distribution (9) obtained from the fit with meson cloud to the pp data read

$$\langle n \rangle[\sqrt{s} = 0.2, 2.76 \text{ TeV}] \approx [2.39, 4.13], \quad (14)$$

$$k[\sqrt{s} = 0.2, 2.76 \text{ TeV}] \approx [0.506, 0.52]. \quad (15)$$

For the scenario without meson cloud $\langle n \rangle = n_{pp}$, and

$$k[\sqrt{s} = 0.2, 2.76 \text{ TeV}] \approx [0.57, 0.57]. \quad (16)$$

As expected, accounting for the meson cloud leads to a reduction of the required fraction of the binary collisions. The effect becomes smaller at the LHC energy. It is due to an increase of the interaction radius from RHIC to LHC, resulting in the lower sensitivity to the internal nucleon structure at the LHC energy.

In Figs. 1, 2 we compare our calculations for the fitted values of α with STAR [22] and ALICE [23] data. The theoretical histograms have been obtained by Monte Carlo generation of $\sim 2 \times 10^6$ events. To illustrate the magnitude of the effect of the meson cloud in Figs. 1a

and 2a we show the results for the scenario without meson cloud obtained with α for the scenario with meson cloud. One can see that at small centrality the meson cloud increases the multiplicity by $\sim 16 - 18\%$. Note that our calculations do not assume a certain internal structure of the bare baryon and meson states. For this reason one can expect that the long range meson-baryon fluctuations in the nucleon wave function should increase the multiplicity in AA collisions in any scheme.

We also studied the effect of meson cloud on the initial anisotropy coefficients ϵ_n ($n = 2 - 5$). We found that the effect of the meson cloud is small (except for very peripheral collisions where the results are not robust due to their sensitivity to the entropy distribution for the wounded constituents and the binary collisions). Recently there was interest in the multiplicity dependence of the ellipticity ϵ_2 for U+U collisions [36, 39, 40]. In [36] it was predicted that due to prolate shape of the ^{238}U nucleus the initial ϵ_2 should have a knee structure at multiplicities in the top 1% U+U collisions related to the growth of the contribution of the binary collisions for the tip-tip configurations of the colliding nuclei. But the elliptic flow v_2 measured by STAR [37, 38] in U+U collisions at $\sqrt{s} = 193$ GeV shows no indication of a knee structure. This challenged the picture with a significant contribution of the binary collisions, and stimulated study of alternative ansatzes for the entropy deposition in the Glauber picture [39, 40]. However, the Glauber calculations of [36] have been performed neglecting the fluctuations of the multiplicity in NN collisions. Later in [42] it was demonstrated that the knee structure vanishes when the fluctuations are taken into account. Our calculations for U+U collisions also show that the knee structure in ϵ_2 is swept out (both with and without meson cloud) when the fluctuations of the sources are taken into account.

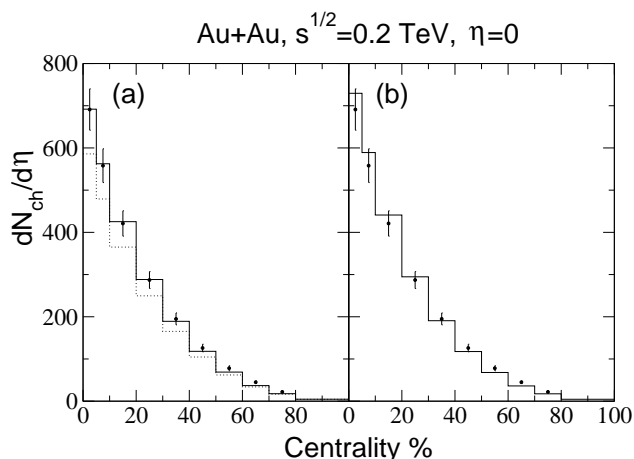


FIG. 1: Centrality dependence of $dN_{ch}/d\eta$ for Au+Au collisions at $\sqrt{s} = 0.2$ TeV. Left: MCG simulation for the scenario with (solid) and without (dotted) meson cloud for $\alpha = 0.06$. Right: MCG simulation for the scenario without meson cloud for $\alpha = 0.135$. Data are from STAR [22].

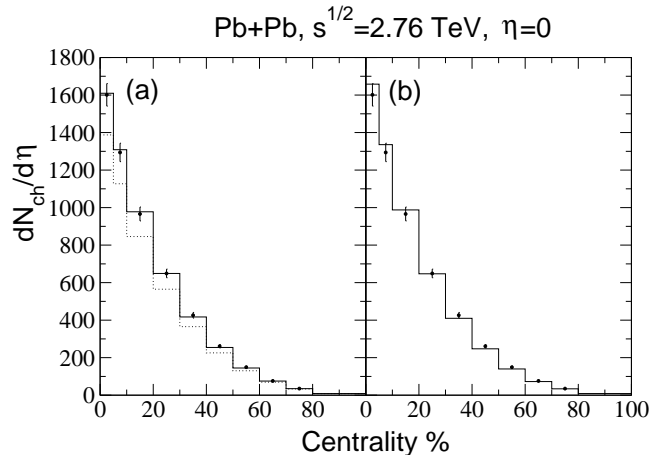


FIG. 2: Centrality dependence of $dN_{ch}/d\eta$ for Pb+Pb collisions at $\sqrt{s} = 2.76$ TeV. Left: MCG simulation for the scenario with (solid) and without (dotted) meson cloud for $\alpha = 0.09$. Right: MCG simulation for the scenario without meson cloud for $\alpha = 0.14$. Data are from ALICE [23].

IV. SUMMARY

We have studied the influence of the meson cloud on predictions of the MCG model for AA collisions. We find that for central AA collisions the meson cloud can increase the multiplicity density in the central rapidity region by $\sim 16 - 18\%$. Accounting for the meson-baryon Fock components of the nucleon reduces the required fraction of the binary collisions by a factor of ~ 2 for Au+Au collisions at $\sqrt{s} = 0.2$ TeV and ~ 1.5 for Pb+Pb collisions at $\sqrt{s} = 2.76$ TeV. One can expect that the observed increase of the multiplicity in AA collisions due to the virtual meson-baryon states in the physical nucleon should exist in other models for the initial conditions in AA collisions.

Acknowledgments

I thank W. Broniowski and S.A. Voloshin for communications. This work is supported in part by the grant RFBR 15-02-00668-a.

References

-
- [1] B. Schenke, P. Tribedy, and R. Venugopalan, Phys. Rev. Lett. **108**, 252301 (2012) [arXiv:1202.6646].
- [2] B. Schenke, P. Tribedy, and R. Venugopalan, Phys. Rev. C **86**, 034908 (2012) [arXiv:1206.6805].
- [3] A. Bialas, M. Bleszynski, and W. Czyz, Nucl. Phys. B **111**, 461 (1976).
- [4] D. Kharzeev and M. Nardi, Phys. Lett. B **507**, 121 (2001) [nucl-th/0012025].
- [5] L.D. McLerran and R. Venugopalan, Phys. Rev. D **49**, 2233 (1994) [hep-ph/9309289].
- [6] E.V. Shuryak, Rev. Mod. Phys. **65**, 1 (1993).
- [7] N.N. Nikolaev and B.G. Zakharov, Z. Phys. C **49**, 607 (1991); *ibid.*, C **53**, 331 (1992).
- [8] R. Fiore, N.N. Nikolaev, and V.R. Zoller, JETP Lett. **99**, 363 (2014) [arXiv:1403.1950].
- [9] B.B. Back *et al.* [PHOBOS Collaboration], Phys. Rev. C **70**, 021902 (2004) [nucl-ex/0405027].
- [10] B.I. Abelev *et al.* [STAR Collaboration], Phys. Rev. C **79**, 034909 (2009) [arXiv:0808.2041].
- [11] M. Rybczynski, W. Broniowski, arXiv:1510.08242.
- [12] B. Alver, M. Baker, C. Loizides, and P. Steinberg, arXiv:0805.4411.
- [13] W. Broniowski, M. Rybczynski, and P. Bozek, Comput. Phys. Commun. **180**, 69 (2009) [arXiv:0710.5731].
- [14] M. Rybczynski, G. Stefanek, W. Broniowski, and P. Bozek, Comput. Phys. Commun. **185**, 1759 (2014) [arXiv:1310.5475].
- [15] A. Bialas, W. Czyz, and W. Furmanski, Acta Phys. Polon. B **8**, 585 (1977).
- [16] A. Bialas and W. Czyz, Acta Phys. Polon. B **10**, 831 (1979).
- [17] P. Bozek, W. Broniowski, and M. Rybczynski, arXiv:1604.07697.
- [18] A. Bialas and A. Bzdak, Phys. Rev. C **77**, 034908 (2008) [arXiv:0707.3720].
- [19] S. Eremín and S. Voloshin, Phys. Rev. C **67**, 064905 (2003) [nucl-th/0302071].
- [20] C. Loizides, arXiv:1603.07375.
- [21] J. Speth and A.W. Thomas, Adv. Nucl. Phys. **24**, 83 (1997).
- [22] B.I. Abelev *et al.* [STAR Collaboration], Phys. Rev. C **79**, 034909 (2009).
- [23] K. Aamodt *et al.* [ALICE Collaboration], Phys. Rev. Lett. **106**, 032301 (2011) [arXiv:1012.1657].
- [24] V.R. Zoller, Z. Phys. C **60**, 141 (1993).
- [25] W. Melnitchouk, J. Speth, and A.W. Thomas, Phys. Rev. D **59**, 014033 (1998) [hep-ph/9806255].
- [26] H. Holtmann, A. Szczurek, and J. Speth, Nucl. Phys. A **596**, 631 (1996) [hep-ph/9601388].
- [27] A.B. Kaidalov and M.G. Poghosyan, Eur. Phys. J. C **67**, 397 (2010) [arXiv:0910.2050].
- [28] A. Capella and E.G. Ferreira, Eur. Phys. J. C **72**, 1936 (2012) [arXiv:1110.6839].
- [29] B. Müller and K. Rajagopal, Eur. Phys. J. C **43**, 15 (2005) [hep-ph/0502174].
- [30] D. Teaney and L. Yan, Phys. Rev. C **83**, 064904 (2011) [arXiv:1010.1876].
- [31] C. Albajar *et al.* [UA1 Collaboration], Nucl. Phys. B **335**, 261 (1990).
- [32] V. Khachatryan *et al.* [CMS Collaboration], JHEP **1002**, 041 (2010) [arXiv:1002.0621].
- [33] V. Khachatryan *et al.* [CMS Collaboration], Phys. Rev. Lett. **105**, 022002 (2010) [arXiv:1005.3299].
- [34] B. Abelev *et al.* [ALICE Collaboration], Eur. Phys. J. C **73**, 2456 (2013) [arXiv:1208.4968].
- [35] K. Aamodt *et al.* [ALICE Collaboration], Eur. Phys. J. C **68**, 89 (2010) [arXiv:1004.3034].
- [36] S.A. Voloshin, Phys. Rev. Lett. **105**, 172301 (2010) [arXiv:1006.1020].
- [37] Y. Pandit [for the STAR collaboration], J. Phys. Conf. Ser. **458**, 012003 (2013) [arXiv:1305.0173].
- [38] L. Adamczyk *et al.* [STAR Collaboration], Phys. Rev. Lett. **115**, 222301 (2015) [arXiv:1505.07812].
- [39] J.S. Moreland, J.E. Bernhard, and S.A. Bass, Phys. Rev. C **92**, 011901 (2015) [arXiv:1412.4708].
- [40] S. Chatterjee *et al.*, arXiv:1510.01311.
- [41] A. Goldschmidt, Z. Qiu, C. Shen, and U. Heinz, arXiv:1502.00603.
- [42] M. Rybczynski, W. Broniowski, and G. Stefanek, Phys. Rev. C **87**, 044908 (2013) [arXiv:1211.2537].